Semiconductor Physics, Quantum Electronics & Optoelectronics, 2024. V. 27, No 4. P. 389-396.

Semiconductor physics

Influence of extended defects on melting behavior of 3C-SiC by molecular dynamics simulations

S. Shmahlii[1] and A. Sarikov[1,2]

[1]*V. Lashkaryov Institute of Semiconductor Physics, National Academy of Sciences of Ukraine,*
41 Nauky Avenue, 03028 Kyiv, Ukraine
[2]*Educational Scientific Institute of High Technologies, Taras Shevchenko National University of Kyiv,*
4-g Hlushkova Avenue, 03022 Kyiv, Ukraine
Correspondence author e-mail: sarikov@isp.kiev.ua (A. Sarikov)

Abstract. The effect of typical extended defects in cubic Si carbide (3C-SiC), namely Shockley partial dislocations and their complexes, on the melting behavior of this material is studied by molecular dynamics simulations. The obtained results evidence a compelling link between the presence of extended defects and the reduction in the 3C-SiC melting temperature. The melting temperature is found to decrease with the concentration of single partial dislocations with the tendency of saturation at ~ 165 K below the respective value for the defect-free material. In their turn, extrinsic partial dislocations reduce the 3C-SiC melting temperature by only about 50 K independently of the concentration, and the effect of triple dislocation complexes is at all negligible. The mechanism of the observed phenomena is discussed in terms of the strain and excess elastic energy introduced by the defects under study. The obtained results have implications for development of 3C-SiC based devices operating at extreme temperatures, from aerospace electronics to thermal protection systems.

Keywords: 3C-SiC, epitaxial layer, extended defect, dislocation, molecular dynamics simulation.

https://doi.org/10.15407/spqeo27.04.389
PACS 61.72.Ff, 61.72.Hh, 61.72.Lk, 61.72.-y, 64.70.dj

Manuscript received 09.09.24; revised version received 06.10.24; accepted for publication 13.11.24; published online 06.12.24.

1. Introduction

3C-SiC is a cubic polytype of Si carbide with substantial potential for application in high-power and high-frequency devices such as low-resistance diodes and MOS transistors [1–5], power electronic converters for electric and hybrid vehicles [6], and inverters and converters for photovoltaic, wind and aircraft turbine applications [7, 8]. Moreover, cubic Si carbide may be a viable option for use in nano-electromechanical systems such as high-frequency oscillators (up to 10 GHz), nanoengines and modulators [9]. Furthermore, 3C-SiC is viewed as a promising material for biosensors and biomedical implants connecting human nervous system to advanced prostheses [10]. These applications of 3C-SiC are enabled by its appropriate mechanical, electronic and thermal properties such as high electron mobility (900 $cm^2/(V\times s)$) and saturation velocity (2×10^7 cm/s), excellent thermal conductivity of 3.2 W/(cm×K) and indirect wide bandgap of about 2.36 eV [11–15]. Since no reliable technological methods to grow 3C-SiC bulk crystals exist, one has to resort to growing 3C-SiC films hetero-epitaxially on Si substrates. A popular modern technology for growing 3C-SiC on Si is based on the idea of a multi-step chemical vapor deposition process [16, 17]. This process begins with substrate preparation involving various cleaning steps and chemical etching or thermal annealing, which result in a flat and atomically clean surface. The next stage is the so-called carbonization, at which a thin 3C-SiC buffer layer is formed on the top of the Si substrate by interaction with a gaseous carbon precursor such as C_3H_8 or C_2H_4. This buffer layer serves to accommodate the lattice mismatch between the Si substrate and the 3C-SiC epitaxial layer. The final stage is the growth of 3C-SiC layer on the top of the carbonized Si substrate at temperatures close to the melting point of silicon (1300–1400 °C) using both Si- (typically, SiH_4) and C-containing precursors.

However, growing 3C-SiC on Si substrates introduces a high amount of structural defects into the epitaxial layers [18, 19] primarily caused by two factors. The first one is a large mismatch (about 20% at room temperature)

© V. Lashkaryov Institute of Semiconductor Physics of the NAS of Ukraine, 2024
© Publisher PH "Akademperiodyka" of the NAS of Ukraine, 2024

in the lattice parameters of 3C-SiC (4.3589 Å) and Si (5.4311 Å) [11]. The second one is the difference in the material thermal expansion coefficients (~ 23% at deposition temperatures and ~ 8% at room temperature) [20]. These defects may be attempted to manipulate by microwave radiation and weak magnetic field treatments as was used for III-V and II-VI semiconductors [21–23]. However, no reliable methods to improve the defect structure of 3C-SiC were proposed so far.

Using cross-section transmission electron microscopy, Mendez *et al.* [24] observed linear misfit dislocations at the interface between the Si substrate and the 3C-SiC epitaxial layer with the density of one dislocation on each five {111} SiC planes. These dislocations were identified as being mainly the Lömer (90° type) ones. However, such misfit dislocations alone are insufficient to fully accommodate the residual strain in the epitaxial layers. Further strain release is achieved by generation of perfect dislocations that dissociate into 30° and 90° Shockley partials connected by stacking faults [25, 26]. At this, the 90° dislocations remain mainly blocked at the 3C-SiC/Si substrate interface during growing the epitaxial film, so that the extended defect structure of the 3C-SiC layers is principally created by propagation and interaction of the 30° dislocations [27, 28]. There have been also indications of multiple stacking faults terminated by dislocation complexes generated by interaction of individual partial dislocations, in 3C-SiC layers. In particular, high-resolution transmission electron microscopy investigations revealed the presence of dislocation complexes made up by two and three partial dislocations at double and triple stacking fault boundaries [29].

Large concentrations of extended defects in 3C-SiC epitaxial layers are expected to influence on all the layer properties including electrical, mechanical and thermal ones. At this, the role of extended defects on modification of the thermal properties is important because of perspective high-temperature applications of this material. In particular, understanding the effect of extended defects and their density on the melting temperature of 3C-SiC may provide a key for predicting and controlling its thermal behavior, which is especially important for applications where high-temperature stability is crucial. To the best knowledge of us, this issue was not addressed before. Lowering the melting point in the presence of defects (both point and planar ones) for metal crystals such as Ni and Al was demonstrated earlier by molecular dynamics simulations [30]. A similar trend was obtained for copper, the melting point of which decreased as the number of vacancies and interstitial defects increased [31]. In this work, we use molecular dynamics simulations to investigate the effect of extended defects and their density on the melting point and pre-melting structural evolution of 3C-SiC. We choose this method because it enables obtaining the dynamic characteristics of materials at the atomic level and at extreme temperatures, which is beyond the capabilities of *in situ* experimental techniques.

2. Method

Molecular dynamics (MD) simulations were performed by the Large-scale Atomic/Molecular Massively Parallel Simulator (LAMMPS) [32] in the isobaric-isothermal (NPT) ensemble. The interactions between the Si and C atoms in the 3C-SiC phase were described by the Vashishta potential [33]. This potential is known for its accurate prediction of extended defects properties and behavior in 3C-SiC, faster defect evolution as compared to other potentials and account for atom interactions beyond the first coordination sphere, which results in a positive stacking fault energy in compliance with the *ab initio* calculations [34]. Periodic boundary conditions were applied to the simulation cells in all three dimensions to mimic the bulk 3C-SiC material evolution. The value of the time step was equal to 2 fs, which was chosen based on energy conservation of the simulation system in preliminary simulation runs. Analysis of the crystalline structure and defect configurations of the cells at different time steps was carried out using the Open Visualization Tool (OVITO) software [35].

To model the effect of extended defects on the melting temperature and pre-melting behavior of the 3C-SiC material, a ca. 171×9×181 Å^3 rectangular-shaped ideal 3C-SiC simulation cell containing 27648 atoms was first prepared. The cell orientation was $[1\bar{1}\bar{2}]$, $[110]$, and $[1\bar{1}1]$ in the directions of the *X*-, *Y*-, and *Z*-axis, respectively. 30° and 90° Shockley partial dislocations were inserted in this cell by displacing all the cell atoms by the following vectors calculated in the framework of the dislocation theory [36]:

$$u_x = \frac{b_{edge}}{2\pi}\left(\tan^{-1}\frac{y}{x} + \frac{xy}{2(1-\nu)(x^2+y^2)}\right), \quad (1)$$

$$u_y = \frac{b_{edge}}{2\pi}\left(\frac{1-2\nu}{4(1-\nu)}\ln\left(x^2+y^2\right) + \frac{xy}{4(1-\nu)(x^2+y^2)}\right), \quad (2)$$

$$u_z = \frac{b_{screw}}{2\pi}\tan^{-1}\frac{y}{x}, \quad (3)$$

where b_{edge} and b_{screw} are the edge and the screw components of the dislocation Burgers vector, respectively, $\nu = 0.25$ is the 3C-SiC Poisson ratio [37], and *x*, *y*, and *z* are the atom coordinates, respectively.

Dislocation dipoles consisting of 30° and 90° Shockley partial dislocation pairs separated by stacking faults were inserted in the $[1\bar{1}1]$ planes. Such defect configurations correspond to the experimentally obtained dipoles resulting from dissociation of perfect 60° dislocations as mentioned in the Introduction section. Moreover, they enable avoiding annihilation of the dislocations during annealing. Pairs of dislocation dipoles with swapped 90° and 30° sequences and opposite dislocation Burgers vectors were always inserted to ensure zero total Burgers vector of all the dislocations in the simulation cell and, hence, to preserve the integrity

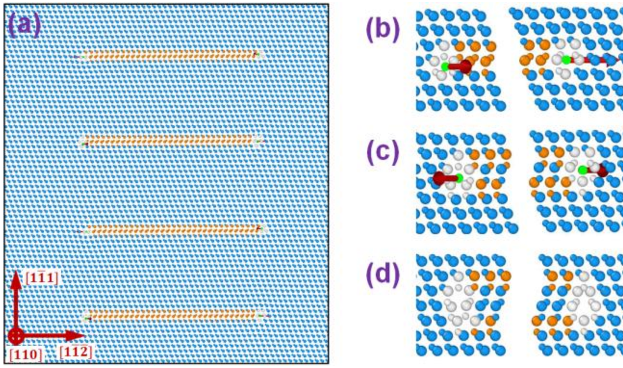

Fig. 1. (a) An exemplary simulation cell with four dislocation dipoles consisting of 30°–90° Shockley partial dislocations separated by stacking faults. (b) Atomic configurations of 30° and 90° Shockley partial dislocations in a dislocation dipole and corresponding Burgers vectors. (c) Atomic configurations of extrinsic partial dislocations and corresponding Burgers vectors. (d) Atomic configurations of triple dislocation complexes with zero Burgers vectors.

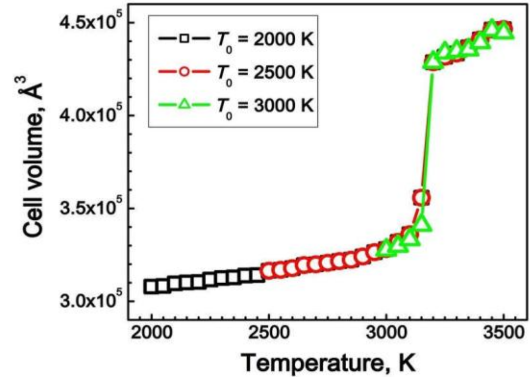

Fig. 2. Temperature dependences of the volume of the 3C-SiC cell with eight partial dislocation dipoles for different starting temperatures of annealing.

of the cell boundaries. The cells with one, two, three and four pairs of 30°–90° dislocation dipoles were prepared to study the effect of the concentration of dislocations on the 3C-SiC melting behavior. An example of a cell with two dipole pairs is shown in Fig. 1a. As can be seen from this figure, the vertical distances between the neighboring dislocation dipole planes were kept the same. Moreover, the distance from the top and the bottom dipole plane to the top and the bottom cell edge, respectively, was set to about half the vertical dipole separation. The horizontal distance from the dislocations to the left and the right cell boundaries was about half the extent of the stacking faults in each dislocation dipole. Such an arrangement allowed equilibrating the interaction forces of the dislocations with the neighboring ones and their images resulting from the periodic boundary conditions.

Furthermore, simulation cells with one, two, three and four dipoles consisting of dislocation complexes made up by 90° and 30° partial dislocations (extrinsic partial dislocations) each as well as one and two dipoles consisting of triple dislocation complexes with zero total Burgers vectors were prepared in a way analogous to the cells with the dislocation dipoles. The atomic configurations of the extrinsic partial dislocations and zero-Burgers-vector triple dislocation complexes are shown in Figs 1b and 1c, respectively. These complexes were found to be stable in 3C-SiC and their formation is favored during the 3C-SiC films growth [38, 39]. Therefore, their possible effect on the thermal behavior of this material should be taken into account as well.

We simulated annealing of all the prepared cells including the ideal one at a step-wise temperature increase (ΔT = 50 K) starting from 2500 K. The cells were annealed during 20 ps at each temperature. This annealing time was chosen to be large enough to enable reaching the steady-state regime of the system on the one hand and to be not too large to affect the total computation time on the other hand. At each temperature, the cell volume was monitored. In accordance with [33], the melting temperature was considered as the one when the cell volume sharply increased as may be seen from Fig. 2. In this figure, the volume of the simulation cell with eight 30°–90° dislocation dipoles (four dipole pairs) *versus* temperature for the starting annealing temperatures of 2000, 2500 and 3000 K is shown. Based on the studies [30, 31], the lowest melting temperature for this system as compared to the systems with smaller defect numbers is expected. Therefore, we have chosen this cell to validate the starting temperature of our simulated anneals. As can be seen from Fig. 2, the melting behavior of the cell does not differ for all three starting temperatures. In this respect, the value of 2500 K was chosen as being sufficiently below the melting temperature on the one hand and ensuring reasonable simulation time on the other hand.

3. Results and discussion

Fig. 3a shows the simulated temperature dependences of the volume of the ideal cell as well as the cells with two, four, six and eight single dislocation dipoles. It can be seen from this figure that the simulated melting temperature corresponding to the sharp increase of the cell volume decreases with the number of dislocation dipoles from 3325 ± 25 K for the ideal cell to 3175 ± 25 K for the cell with eight dipoles. It should be noted that the simulated melting temperature for the ideal cell has a reasonable agreement with the corresponding value of 3250 ± 50 K obtained by molecular dynamics simulations for a different cell size [33] as well as with the experimental value of ~ 3103 K [40], which supports the reliability of the obtained results. It can be further seen from Fig. 3a that the higher is the concentration of dislocation dipoles in the cell, the lower is the rate of the melting temperature decrease pointing to a tendency of saturation at high dislocation concentrations.

Fig. 3b demonstrates the simulated effect of extrinsic partial dislocations on the 3C-SiC melting temperature. It can be seen from this figure that the temperature dependences of the volume of the cells with inserted one, two, three and four extrinsic partial

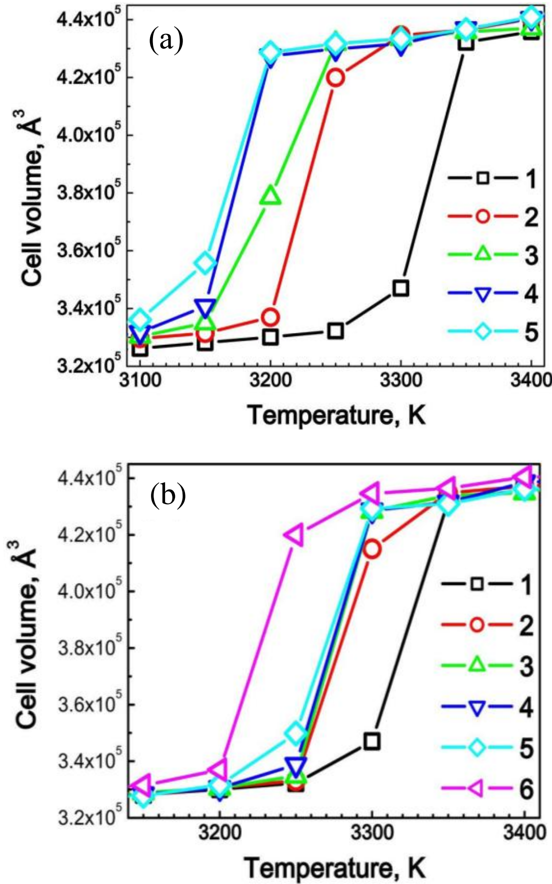

Fig. 3. (a) Temperature dependences of the volume of the ideal 3C-SiC cell (*1*) as well as the cells with two (*2*), four (*3*), six (*4*) and eight (*5*) partial dislocation dipoles. (b) Temperature dependences of the volume of the 3C-SiC cell with one (*2*), two (*3*), three (*4*) and four (*5*) extrinsic partial dislocation dipoles. For comparison, the temperature dependences of the volume of the ideal cell (*1*) and the cell with two partial dislocation dipoles (*6*) are also shown.

dislocation dipoles overlap, which indicates no noticeable impact of such dislocation density on the melting behavior. Besides, the melting temperature of the cells with extrinsic partial dislocations amounts to 3275 ± 25 K, which is higher than the respective value for the cell with the smallest number of partial dislocation dipoles (two), studied in this work. This means that the effect of extrinsic partial dislocations is anyways smaller as compared to that provided by single dislocations. Finally, the results of the simulations for the cells with inserted one and two dipoles containing triple dislocation complexes show no difference in the melting temperature of such cells from that of the ideal cell, which indicates vanishingly small effect of triple dislocation complexes on the 3C-SiC melting behavior. These results are summarized in Fig. 4. It can be seen from this figure that the dependence of the cell melting temperature on the number of single dislocation dipoles in it may be approximated by the following analytical function:

$$T = 159.3 \cdot \exp(-0.384N) + 3160, \qquad (4)$$

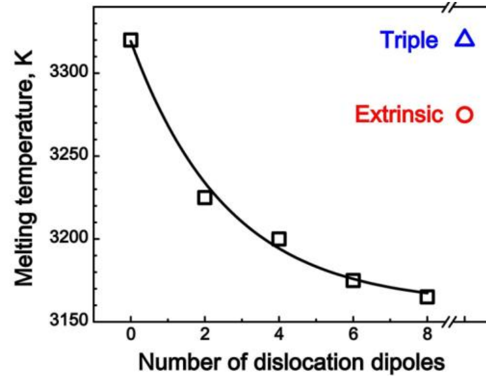

Fig. 4. Melting temperature *versus* number of partial dislocation dipoles in the cell. The molecular dynamics simulation results are shown by symbols and the line is approximation by the expression (4). In addition, the melting temperatures of the cells with extrinsic partial dislocations and triple dislocation complexes are indicated.

where T is the temperature and N is the number of dislocation dipoles in the cell, respectively. The obtained results allow one to conclude that high concentrations of partial dislocations in 3C-SiC would induce a decrease in its melting temperature by up to ~ 200 K ($T \to 3160$ K at $N \to \infty$). At the same time, extrinsic partial dislocations cause substantially smaller decrease in the melting temperature, by about 50 K, independently on their concentration, while the effect by triple dislocation complexes is at all negligible.

To get an insight into the mechanisms defining the observed dependences of the 3C-SiC melting temperature on the type and concentration of extended defects under study, we considered the evolution of the cell dislocation structures with temperature in more detail. Fig. 5 shows simulated snapshots of the exemplary cell with four dislocation dipoles at the temperatures approaching the melting point. It can be seen from this figure that the crystal structure at the dislocation cores starts to destroy at much lower temperatures as compared to the ideal lattice (see the top panels of Fig. 5), *i.e.* dislocation cores are the centers of heterogeneous nucleation for crystalline-to-amorphous transformation. The formed disordered regions expand to the rest of the crystal with the increase in temperature as shown in the bottom panels of Fig. 5 finally leading to complete cell amorphization. Such behavior is reasonable to attribute to the strain and associated stress induced in the crystal lattice by the dislocation cores. As a result, the energy barrier for phase transition from the crystalline to the amorphous state is reduced leading to the decrease in the melting temperature.

To verify this hypothesis, we investigated the distribution of strain and elastic energy in the cells with different types and concentrations of dislocations. Fig. 6 illustrates the maps of volumetric strain as well as elastic energy density in the exemplary 3C-SiC cells with two partial dislocation dipoles (Figs 6a and 6b), two extrinsic partial dislocation dipoles (Figs 6c and 6d) and two dipoles consisting of triple dislocation complexes (Figs 6e and 6f).

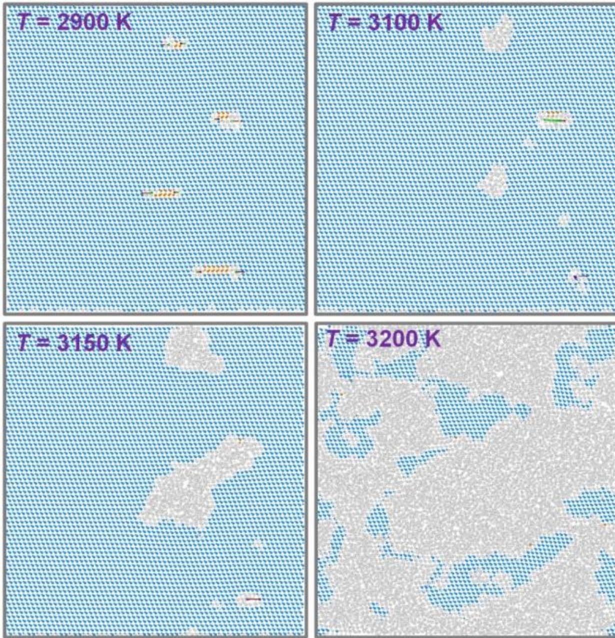

Fig. 5. Snapshots of the simulation cell with four partial dislocation dipoles showing the pre-melting evolution of the 3C-SiC crystal structure.

As can be seen from this figure, the strain introduced by single dislocations and, hence, the corresponding elastic energy density are the highest among the studied cases. These values decrease with the increase in the number of dislocations in the dislocation complexes. Our earlier studies demonstrate that the tendency of reducing strain and excess elastic energy constitutes the formation mechanism of double and triple dislocation complexes from single dislocations during 3C-SiC film growth [38, 39]. The strain and excess energy fields created by single dislocations are long-range, overlapping for neighboring dislocations and affecting the entire 3C-SiC bulk structure. The intensities of these fields in the crystal bulk strongly depend on the concentration of dislocations at their low values (hence, large distances between them). This dependence becomes weaker as the dislocation concentration increases finally leading to the state when adding one dislocation dipole hardly influences the effect of strain and stress induced by already present dislocations. This mechanism explains the observed dependence of the rate of melting temperature decrease on the number of dislocation dipoles in the cell, when this rate is the highest at small numbers of dislocation dipoles, decreases upon raising this number and finally tends to saturate at $N \to \infty$. On the other hand, the strain and excess elastic energy induced by the extrinsic partial dislocations span for only several neighboring atomic shells around the dislocation cores, while the triple dislocation complexes affect only the core nearest-neighbors, as can be seen from Figs 6c–6f. Such findings explain the much smaller impact of extrinsic partial dislocations on the 3C-SiC melting temperature as compared to the effect of single dislocations, and its independence on the dislocation concentration as well as the negligible influence on the melting temperature of triple dislocation complexes.

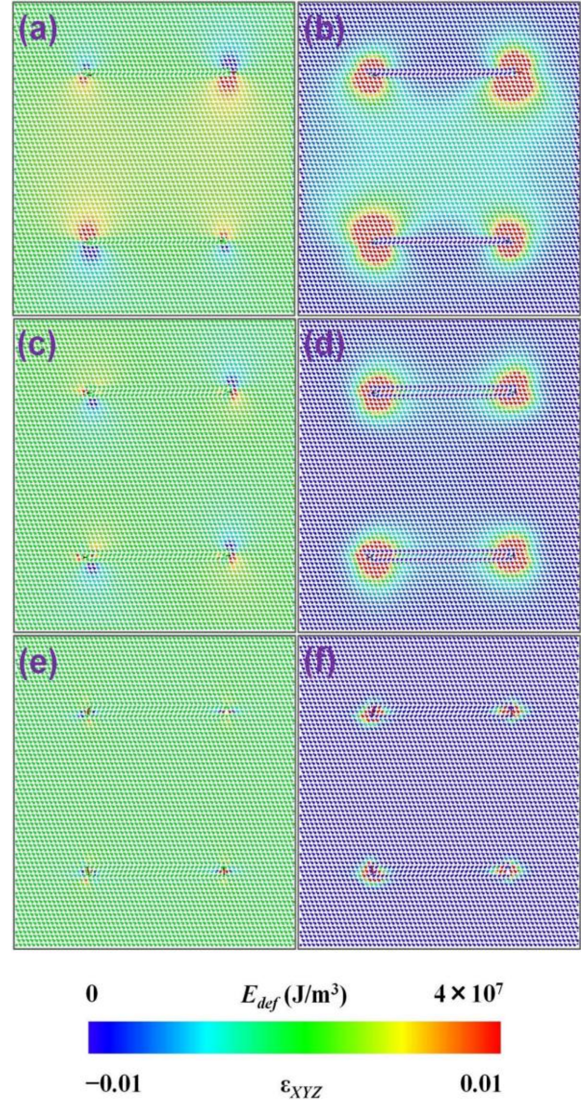

Fig. 6. Distribution of volumetric strain (a, c, e) and elastic energy density (b, d, f) in the 3C-SiC cells with two partial dislocation dipoles (a, b), two extrinsic partial dislocation dipoles (c, d), and two dipoles consisting of triple dislocation complexes (e, f).

The obtained decrease of the melting temperature of 3C-SiC caused by extended defects and understanding its mechanisms are important not only from the point of view of expanding the fundamental knowledge about the material properties but also have implications for device application of this material. As was already mentioned in the Introduction section, a modern technology uses growing 3C-SiC epitaxial layers on Si substrates with large lattice mismatch of about 20% [11]. Such growth conditions favor formation of high concentrations of extended defects, especially partial dislocations and dislocation complexes, in the 3C-SiC layers [18, 19, 28]. Understanding thermal behavior of the real defect-rich 3C-SiC is vital for designing and predicting functionality of 3C-SiC based devices especially those intended for operation at extreme temperatures. In particular, such devices include jet engine control electronics and sensors for aerospace applications, which should be placed as close as possible

to the fuel combustion zone with the temperature reaching ~2000 °C [41]. The SiC based extreme temperature electronics is also demanded on the space-crafts operating in the vicinity of the Sun to significantly reduce shielding and heat dissipation installations and, hence, the spacecraft weight [42]. Moreover, such electronics may be also used to control the performance of nuclear reactors on future spaceships for exploiting the outer solar system [43]. Tolerance of the SiC circuits to the action of high temperatures will make possible reduction of their shielding and allow placing them closer to the control areas. Furthermore, non-electronic applications of Si carbide such as for ceramic matrix composites for aerospace and gas turbine engines also rely on material properties at the temperatures near the melting points of their components [44]. The discovered modification of the melting temperature due to the presence of extended defects hints that the temperature-dependent characteristics such as electrical, optical, and elastic ones, of the real 3C-SiC may be affected as compared to those of the ideal material causing degradation of the electronics operating at extremely high temperatures and voltages. In our forthcoming publications, the effect of extended defects on the mentioned characteristics of 3C-SiC material will be considered in detail.

We may compare now our findings with the respective results known from the literature. A number of publications were devoted to the studies of the influence of different types of defects in various materials on their melting points. It was demonstrated in particular [45] that introduction of 1.47% of vacancy clusters reduces the glass transition temperature of amorphous Si by about 12.4%. In [46], modelling the melting transition of vanadium by molecular dynamics simulations, the authors detected the effect of interstitials and vacancies on its melting temperature. They found out that increase of the concentration of interstitials up to 1.2% shifted the melting point from 2500 to 2360 K, while increase of the vacancy concentration up to 1.2% decreased it by only about 20 K. Molecular dynamics simulations also revealed a decrease of the melting temperature of metal crystals such as Ni, Al, and Cu with the concentration of point and planar defects [30, 31]. We may conclude therefore that the melting behavior of 3C-SiC obtained in our simulations has a good agreement with the patterns known for other materials, for which presence of extended defects reduces the melting temperature and the extent of their impact strongly depends on the defect type and material in question.

4. Conclusion

In this work, the effect of typical extended defects in 3C-SiC on its melting temperature is studied by molecular dynamics simulations. Single partial dislocations are revealed to have a much stronger influence on the 3C-SiC melting properties than the complexes consisting of two and three partial dislocations. The melting temperature is found to decrease with the concentration of single dislocations finally tending to saturate at the value about 165 K below the melting point of the ideal crystal. On the other hand, presence of extrinsic partial dislocations reduces the 3C-SiC melting temperature by only ~ 50 K independently on their concentration, while the effect of triple dislocation complexes is at all negligible. The mechanism of the observed phenomena is attributed to the defect-induced strain and excess elastic energy and difference in their values for single dislocations and dislocation complexes. The obtained results may be useful for the researchers and industries focusing on the development of 3C-SiC based harsh thermal environment electronics and thermal protection systems to enhance the efficiency and safety of their products as well as to expand the temperature range of their operation.

Funding: This research received no external funding.

Data Availability Statement: Data are available on request.

Conflicts of Interest: The authors declare no conflicts of interest.

References

1. Li F., Roccaforte F., Greco G. *et al.* Status and prospects of cubic silicon carbide power electronics device technology. *Materials*. 2021. **14**. P. 5831. https://doi.org/10.3390/ma14195831.
2. Anzalone R., Privitera S., Camarda M. *et al.* Interface state density evaluation of high quality hetero-epitaxial 3C-SiC(001) for high-power MOSFET applications. *Mater. Sci. Eng. B*. 2015. **198**. P. 14–19. https://doi.org/10.1016/j.mseb.2015.03.014.
3. Lee K.K., Pensl G., Soueidan M. *et al.* Very low interface state density from thermally oxidized single-domain 3C-SiC/6H-SiC grown by vapour–liquid–solid mechanism. *Jpn. J. Appl. Phys*. 2006. **45**. P. 6823. https://doi.org/10.1143/JJAP.45.6823.
4. Schöner A., Krieger M., Pensl G. *et al.* Fabrication and characterization of 3C-SiC-based MOSFETs. *Chem. Vapor Dep*. 2006. **12**. P. 523. https://doi.org/10.1002/cvde.200606467.
5. Li F., Sharma Y.K., Fisher C.A. *et al.* A novel 3C-SiC on Si power Schottky diode design and modelling. *MRS Online Proc. Lib*. 2014. **1693**. P. 93–98. https://doi.org/10.1557/opl.2014.571.
6. Chatterjee P., Hermwille M. Tackling the challenges of electric vehicle fast charging. *ATZ Electron. Worldwide*. 2020. **15**. P. 18–22. https://doi.org/10.1007/s38314-020-0263-6.
7. Schefer H., Fauth L., Kopp T.H. *et al.* Discussion on electric power supply systems for all electric aircraft. *IEEE Access*. 2020. **8**. P. 84188–84216. https://doi.org/10.1109/ACCESS.2020.2991804.
8. Zhang H., Tolbert L.M. Efficiency impact of silicon carbide power electronics for modern wind turbine full scale frequency converter. *IEEE Trans. Ind. Electron*. 2011. **58**. P. 21–28. https://doi.org/10.1109/TIE.2010.2048292.
9. Huang X.M.H., Zorman C.A., Mehregany M., Roukes M.L. Nanodevice motion at microwave frequencies. *Nature*. 2003. **421**. P. 496. https://doi.org/10.1038/421496a.
10. Saddow S.E., Frewin C.L., Nezafati M., Oliveros A. 3C-SiC on Si: a bio- and hemo- compatible material

for advanced nano-bio devices. In: *Proc. 2014 IEEE 9th Nanotechnol. Mater. and Devices Conf.* (*NMDC*), Aci Castello, Italy, 13–15 October 2014. P. 49–53. https://doi.org/10.1109/NMDC.2014.6997419.

11. Ruff M., Mitlehner H., Helbig R. SiC devices: physics and numerical simulation. *IEEE Trans. Electron. Dev.* 1994. **41**. P. 1040–1054. https://doi.org/10.1109/16.293319.
12. Harris G.L. *Properties of Silicon Carbide*. INSPEC, the Institution of Electrical Engineers, London, 1995.
13. Morkoç H., Srite S., Gao G.B. *et al.* Large-band-gap SiC, III-V nitride, and II-VI ZnSe-based semiconductor device technologies. *J. Appl. Phys.* 1994. **76**. P. 1363–1398. https://doi.org/10.1063/1.358463.
14. Casady J., Johnson R. Status of silicon carbide (SiC) as a wide-bandgap semiconductor for high-temperature applications: a review. *Solid-State Electr*. 1996. **39**. P. 1409–1422. https://doi.org/10.1016/0038-1101(96)00045-7.
15. Saddow S.E., Agarwal A.K. Advances in silicon carbide processing and applications. *BioMed. Eng. OnLine.* 2005. **4**. P. 33. https://doi.org/10.1186/1475-925X-4-33.
16. Ferro G. 3C-SiC heteroepitaxial growth on silicon: the quest for Holy Grail. *Critical Rev. in Solid State and Mater. Sci.* 2015. **40**. P. 56–76. https://doi.org/10.1080/10408436.2014.940440.
17. Nishiguchi T., Nakamura M., Nishio K. *et al.* Heteroepitaxial growth of (111) 3C-SiC on well-lattice-matched (110) Si substrates by chemical vapor deposition. *Appl. Phys. Lett.* 2004. **84**. P. 3082–3084. https://doi.org/10.1063/1.1719270.
18. La Via F., Severino A., Anzalone R. *et al.* From thin film to bulk 3C-SiC growth: Understanding the mechanism of defects reduction. *Mater. Sci. Semicond. Proc*. 2018. **78**. P. 57–68. https://doi.org/10.1016/j.mssp.2017.12.012.
19. Zimbone M., Sarikov A., Bongiorno C. *et al.* Extended defects in 3C-SiC: Stacking faults, threading partial dislocations, and inverted domain boundaries. *Acta Mater.* 2021. **213**. P. 116915. https://doi.org/10.1016/j.actamat.2021.116915.
20. Slack G.A., Bartram S.F. Thermal expansion of some diamondlike crystals. *J. Appl. Phys.* 1975. **46**. P. 89–98. https://doi.org/10.1063/1.321373.
21. Redko R.A., Konakova R.V., Milenin V.V. *et al.* Long-term transformation of GaN/Al_2O_3 defect subsystem induced by weak magnetic fields. *J. Lumin*. 2014. **153**. P. 417–420. https://doi.org/10.1016/j.jlumin.2014.03.068.
22. Milenin G.V., Redko R.A. Transformation of structural defects in semiconductors under action of electromagnetic and magnetic fields causing resonant phenomena. *SPQEO*. 2019. **22**. P. 39–46. https://doi.org/10.15407/spqeo22.01.039.
23. Redko R.A., Budzulyak S.I., Vakhnyak N.D. *et al.* Effect of microwave (24 GHz) radiation treatment on impurity photoluminescence of CdTe:Cl single crystals. *J. Lumin.* 2016. **178**. P. 68–71. https://doi.org/https://doi.org/10.1016/j.jlumin.2016.05.032.
24. Mendez D., Aouni A., Morales F.M. *et al.* Defect morphology and strain of CVD grown 3C-SiC layers: effect of the carbonization process. *phys. status solidi* (*a*). 2005. **202**. P. 561–565. https://doi.org/10.1002/pssa.200460421.
25. Kaiser U., Khodos I. On the determination of partial dislocation Burgers vectors in fcc lattices and its application to cubic SiC films. *Phil. Mag. A*. 2002. **82**. P. 541–551. https://doi.org/10.1080/01418610208239615.
26. Wen C., Wang Y.M., Wan W. *et al.* Nature of interfacial defects and their roles in strain relaxation at highly lattice mismatched 3C-SiC/Si (001) interface. *J. Appl. Phys*. 2009. **106**. P. 073522. https://doi.org/10.1063/1.3234380.
27. Sarikov A., Marzegalli A., Barbisan L. *et al.* Mechanism of stacking fault annihilation in 3C-SiC epitaxially grown on Si(001) by molecular dynamics simulations. *CrystEngComm.* 2021. **23**. P. 1566–1571. https://doi.org/10.1039/D0CE01613F.
28. La Via F., Zimbone M., Bongiorno C. *et al.* New approaches and understandings in the growth of cubic silicon carbide. *Materials*. 2021. **14**. P. 5348. https://doi.org/10.3390/ma14185348.
29. Lancin M., Ragaru C., Godon C. Atomic structure and core composition of partial dislocations and dislocation fronts in β-SiC by high-resolution transmission electron microscopy. *Phil. Mag. B*. 2001. **81**. P. 1633–1647. https://doi.org/10.1080/13642810108223108.
30. Hussain F., Hayat S.S., Shah Z.A., Ahmad S.A. Effect of crystal defects on the melting temperature of Ni and Al. *Chin. J. Phys.* 2013. **51**. P. 347–358. https://doi.org/10.6122/CJP.51.347.
31. Kamani S.K. *Influence of defects on thermal and mechanical properties of metals*, Master thesis, Texas A&M University, USA, 15 May 2009.
32. Plimpton S. Fast parallel algorithms for short-range molecular dynamics. *J. Comp. Phys.* 1995. **117**. P. 1–19. https://doi.org/10.1006/jcph.1995.1039.
33. Vashishta P., Kalia R.K., Nakano A., Rino J.P. Interaction potential for silicon carbide: A molecular dynamics study of elastic constants and vibrational density of states for crystalline and amorphous silicon carbide. *J. Appl. Phys*. 2007. **101**. P. 103515. https://doi.org/10.1063/1.2724570.
34. Sarikov A., Marzegalli A., Barbisan L. *et al.* Molecular dynamics simulations of extended defects and their evolution in 3C-SiC by different potentials. *Model. Simul. Mater. Sci. Eng.* 2019. **28**. P. 015002. https://doi.org/10.1088/1361-651X/ab50c7.
35. Stukowski A. Visualization and analysis of atomistic simulation data with OVITO – the open visualization tool. *Model. Simul. Mater. Sci. Eng.* 2010. **18**. P. 015012. https://doi.org/10.1088/0965- 0393/18/1/015012.
36. Hirth J., Lothe J. *Theory of Dislocations*, 2nd ed. Krieger Publishing Company, Malabar, FL, 1982.
37. Tong L., Mehregany M., Matus L.G. Mechanical properties of 3C silicon carbide. *Appl. Phys. Lett.* 1992.

60. P. 2992–2994. https://doi.org/10.1063/1.106786.
38. Sarikov A., Marzegalli A., Barbisan L. *et al.* Structure and stability of partial dislocation complexes in 3C-SiC by molecular dynamics simulations. *Materials*. 2019. **12**. P. 3027. https://doi.org/10.3390/ma12183027.
39. Scalise E., Barbisan L., Sarikov A. *et al.* The origin and nature of killer defects in 3C-SiC for power electronic applications by a multiscale atomistic approach. *J. Mater. Chem. C*. 2020. **8**. P. 8380–8392. https://doi.org/10.1039/d0tc00909a.
40. Kleykamp H., Schumacher G. The constitution of the silicon-carbon system. *Ber. Bunsenges. Phys. Chem*. 1993. **97**. P. 799–804. https://doi.org/10.1002/bbpc.19930970609.
41. Quigley R. More electric aircraft. In: *Proc. Eighth Annual Applied Power Electronics Conf. and Exposition* (*APEC*), San Diego, California, USA, 07–11 March 1993. P. 906–911. https://doi.org/10.1109/APEC.1993.290667.
42. La Via F., Alquier D., Giannazzo F. *et al.* Emerging SiC applications beyond power electronic devices. *Micromachines*. 2023. **14**. P. 1200. https://doi.org/10.3390/mi14061200.
43. Mason L.S. A comparison of energy conversion technologies for space nuclear power systems. In: *Proc. Int. Energy Conversion Eng. Conf*., Cincinnati, Ohio, USA, 9–11 July 2018. https://doi.org/10.2514/6.2018-4977.
44. Fenetaud P., Jacques S. SiC/SiC ceramic matrix composites with BN interphase produced by gas phase routes: an overview. *Open Ceram*. 2023. **15**. P. 100396. https://doi.org/10.1016/j.oceram.2023.100396.
45. Ji H., Wang X., Li H. *et al.* A molecular dynamics simulation of the influence of defect on the melting of amorphous silica. In: *Proc. Second Int. Conf. on Mater. Chem. and Environ. Protection (MEEP2018)*, Sanya City, China, 23–25 November 2018. P. 193–198. https://doi.org/10.5220/0008187501930198.
46. Sorkin V., Polturak E., Adler J. Molecular dynamics study of melting of the bcc metal vanadium. I. Mechanical melting. *Phys. Rev. B*. 2003. **68**. P. 174102. https://doi.org/10.1103/physrevb.68.174102.

Authors and CV

Serhii Shmahlii, Junior Researcher at the V. Lashkaryov Institute of Semiconductor Physics, NAS of Ukraine. Author of 4 publications. The area of his scientific interests includes atomistic modelling of properties and transformations of semiconductor structures.

Andrey Sarikov, Doctor of Sciences (Physics and Mathematics), Leading Researcher at the V. Lashkaryov Institute of Semiconductor Physics, NAS of Ukraine and Associate Professor at the Educational Scientific Institute of High Technologies, Taras Shevchenko National University of Kyiv. Author of over 120 publications. The area of his scientific interests includes study of the processes of formation and transformations of semiconductor based structures by numerical, Monte Carlo and molecular dynamics simulations. https://orcid.org/0000-0001-9123-7203

Authors' contributions

Shmahlii S.: software, formal analysis, investigation, data curation, writing – original draft preparation.

Sarikov A.: conceptualization, methodology, writing – review and editing, supervision.

All authors have read and agreed to the published version of the manuscript.

Вплив протяжних дефектів на процес плавлення 3C-SiC, отриманий моделюванням методом молекулярної динаміки

С. Шмаглій та А. Саріков

Анотація. З використанням методу молекулярної динаміки досліджено вплив типових протяжних дефектів у кубічному карбіді кремнію (3C-SiC), а саме часткових дислокацій Шоклі та їх комплексів, на процес плавлення цього матеріалу. Отримані результати свідчать про чіткий зв'язок між наявністю протяжних дефектів та зниженням температури плавлення 3C-SiC. Встановлено, що температура плавлення знижується зі зростанням концентрації часткових дислокацій з тенденцією до насичення на рівні ~ 165 K нижче за відповідне значення для бездефектного матеріалу. У свою чергу часткові дислокації впровадження приводять до зниження температури плавлення 3C-SiC приблизно на 50 K незалежно від їх концентрації, у той час як ефект, викликаний присутністю потрійних дислокаційних комплексів, є незначним. Механізм спостережуваних явищ обговорено в термінах деформації та надлишкової пружної енергії, спричинених досліджуваними дефектами. Отримані результати мають значення для розробки пристроїв на основі 3C-SiC для роботи при екстремальних температурах – від приладів аерокосмічної електроніки до систем теплового захисту.

Ключові слова: 3C-SiC, епітаксійний шар, протяжний дефект, дислокація, моделювання методом молекулярної динаміки.